Surface & Coatings Technology 385 (2020) 125368

Contents lists available at ScienceDirect

Surface & Coatings Technology

journal homepage: www.elsevier.com/locate/surfcoat

(100) oriented diamond film prepared on amorphous carbon buffer layer containing nano-crystalline diamond grains

Yunxiang Lu[a,b,1], Weidong Man[a,*], Bo Wang[b,*,1], Andreas Rosenkranz[c], Mingyang Yang[b], Ke Yang[b], Jian Yi[b], Hui Song[b], He Li[b], Nan Jiang[b]

[a] Provincial Key Laboratory of Plasma Chemistry and Advanced Materials, Wuhan Institute of Technology, Wuhan 430073, People's Republic of China
[b] Key Laboratory of Marine New Materials and Related Technology, Zhejiang Key Laboratory of Marine Materials and Protection Technology, Ningbo Institute of Material Technology & Engineering, Chinese Academy of Sciences, Ningbo 315201, People's Republic of China
[c] Department of Chemical Engineering, Biotechnology and Materials, Universidad de Chile, Avenida Beauchef 851, Santiago, Chile

ARTICLE INFO

Keywords:
(100) oriented diamond films
Single crystal diamond plate
Amorphous carbon buffer layer
Lateral growth
Transmission electron microscopy

ABSTRACT

In this study, amorphous carbon buffer layer containing nano-crystalline diamond grains was pre-deposited on single crystal silicon (Si) wafers. (100) oriented diamond films were prepared on the buffer layer by increasing deposition temperature. Morphology observation demonstrated that (100) oriented diamond plates appear on the buffer layer, thus realizing the deposition of (100) oriented diamond film. Transmission electron microscopy confirmed that (100) oriented diamond dominates deposition at high temperatures, leading to the formation of the (100) oriented diamond plates. The fast lateral growth of nano-crystalline diamond grains with (100) orientation in the buffer layer is the main driving force for the deposition of (100) oriented diamond film, providing a new route for the preparation of (100) oriented diamond films.

1. Introduction

The surface morphology of diamond films has a significant influence on its performance, which is particularly important in different fields such as tribology, machinability, optics, electricity and wettability [1–11]. Therefore, the surface morphology of diamond films remains to be intensively investigated since chemical vapor deposition (CVD) diamond films have been developed. Several factors contribute to the surface morphology of diamond films. Among them, the growth orientation of diamond grains plays an important role related to the surface morphology. There are three common orientations for diamond, namely (111), (110) and (100) orientations [11,12]. Shapes of diamond grains with different orientations have been discussed well in previous researches. (100) oriented diamond film possesses the lowest surface roughness among the three different orientations, benefiting from its square surface. Compared to (111) and (110) facets, this makes (100) oriented diamond films more suitable for tribological, optical and electrical applications [11].

In previous studies, various methods have been proposed to deposit (100) oriented diamond films [3,8,11,13–22]. The orientation of polycrystalline films and the shape of isolated grains was efficiently controlled through adjusting the deposition conditions [1,14,17,28]. (111) oriented diamond grains were usually achieved at lower methane concentrations, whereas diamond grains deposited at higher methane concentrations often exhibit (100) orientation [11]. Besides, the deposition temperature has a great influence on the growth orientation of diamond [3,22]. Highly oriented diamond films have also been prepared by assisted CVD technologies, such as alternating current substrate bias, lower-than-normal filament temperature pretreatment, bias enhanced nucleation (BEN) and thermal carburization [16,19,20,22]. However, (100) oriented diamond films prepared by these methods often have a low compactness, resulting from pores among large diamond grains. Additonally, the deposition mechanism of highly oriented diamond films is still unclear due to the missing experimental evidences at nanoscale. Morphology observation and X-ray diffraction have been employed to explain the growth of oriented diamond film [1,12,14]. However, these methods have not fully revealed the fundamental growth mechanism of the highly oriented diamond films [23]. Therefore, it is imperative to prepare compact (100) oriented diamond film and investigate its deposition mechanism.

In this work, (100) oriented diamond films were deposited on amorphous carbon buffer layer containing nano-crystalline diamond grains using a microwave CVD device (MPCVD). Scanning electron microscopy (SEM) observation demonstrated that the diamond plates

* Corresponding authors.
E-mail addresses: 38838515@qq.com (W. Man), wangb@nimte.ac.cn (B. Wang).
[1] Y.X. Lu and B. Wang contributed equally to this work.

https://doi.org/10.1016/j.surfcoat.2020.125368
Received 22 July 2019; Received in revised form 4 December 2019; Accepted 13 January 2020
Available online 21 January 2020

appear on the amorphous carbon buffer layers and the diamond films exhibit (100) orientation. Moreover, the microstructure evolution of single diamond plates on the (100) oriented diamond film has been observed using transmission electron microscopy (TEM).

2. Experimental details

Single-side polished N (100) Si wafers with a thickness of 2 mm and an area of 15 × 15 mm^2 were used as substrates. The Si substrates were mechanical scratched with diamond powders of 1 μm in diameter. Afterwards, the substrates were seeded through ultrasonication treatment in an acetone solution containing ultrafine diamond powders (100 nm in diameter) for 10 min. Subsequently, the Si wafers were cleaned with ethyl alcohol to remove residual diamond powders on the wafer surface and dried with compressed air.

Amorphous carbon buffer layers containing nano-crystalline diamond grains were pre-deposited on the seeded Si wafers using a MPCVD device. The MPCVD device is mainly comprised of microwave source, reactor, air intake, water cooling plate. In diamond deposition process, the mixed gas containing methane and hydrogen is input in the reactor and decomposed into plasma under the microwave produced by the microwave plasma source. The deposition temperature was controlled through adjusting the power of the microwave source. Pre-deposition temperature and duration were kept constant at 900 °C and 8 h, respectively. (100) diamond films were prepared on the amorphous carbon buffer layers containing nano-crystalline diamond grains at 920, 940 and 960 °C respectively, through changing growth powers from 2.0 to, 2.3 and 2.5 kW. All pre-deposition and deposition processes were conducted in a gas mixture of methane and hydrogen with flow rates of 10 and 400 standard cubic centimeters per minute (sccm), respectively. Growth durations were kept constant at 8 h for all samples.

The temperature of substrate was measured by a portable radiation thermometer (CHINO, IR-AH, Japan). Surface morphology of specimens was examined by SEM (Thermo scientific, Verios G4 UC, USA). The Raman spectra of diamond were measured by Confocal micro-Raman spectrometer (Renishaw, inVia Reflex) with a laser wavelength of 532 nm. The cross-sectional TEM sample was prepared on a single diamond plate deposited at 960 °C using focused ion beam microscopy (FIB, Carl Zeiss, Auriga, Germany). The TEM sample was cut along the diagonal direction of the single diamond plate. The microstructure of diamond was characterized in detail by TEM (ThemoFisher, Talos F200x, England) operated at an accelerated voltage of 200 kV. Tribological tests were performed by a ball-on-disk tribometer (TRB3, Anton Paar, Austria) operating in a linear reciprocating mode. For the measurement, normal load, sliding speed and stroke length were 2 N, 20 mm/s and 5 mm, respectively. A Si_3N_4 ball of 6 mm in diameter was used as a sliding counterbody. Nanoindentation experiments were carried out using a Nano Indenter XP (MTS Systems, G200, USA) equipped with a standard Berkovich indenter. Indentation depth is 2 μm, which is < 10% of the film thickness. The maximum load applied on the sample was 650 mN.

3. Results and discussion

Fig. 1 shows the SEM micrographs of the pre-deposited buffer layer and diamond films deposited on the buffer layer at different temperatures. As illustrated in Fig. 1a, sharp micron-scale pyramid-shaped clusters can be clearly seen in the film grown at 900 °C. From the inset in Fig. 1a, it becomes obvious that every pyramid-shaped cluster consists of numerous nano-crystalline diamond grains. However, diamond plates appeared at the top of the octahedron-shaped clusters after increasing the deposition temperature to 920, 940 and 960 °C, as can be observed in Fig. 1 b-d, which is responsible for the (100) orientation of the diamond films. For the deposition temperature of 920 °C, the plates have side lengths of about 1 μm, as illustrated in the inset of Fig. 1b. The size of plates becomes larger with increasing deposition temperature. As the deposition temperature reached 960 °C, the plates almost cover the entire film surface and even overlap each other, forming a compact diamond film of (100) orientation. The average plate size depending on deposition temperature is calculated in SEM images. The average values of side lengths for diamond plates formed at 920, 940 and 960 °C were 1.34, 3.01 and 6.12 μm, respectively.

Fig. 2 displays the Raman spectra of the diamond films grown at different temperatures. The characteristic peaks of diamond can be clearly observed at 1332 cm^{-1} in all curves (Fig. 2a). However, broad peaks at 1430 cm^{-1} were identified in the Raman spectra for diamond films deposited at 920 and 940 °C. The weak peak at 1430 cm^{-1} can be associated to the nano-crystalline diamond in the buffer layer [24]. Regarding the spectrum of the diamond film deposited at 900 °C, there exists another broad peak at 1515 cm^{-1}. It can be traced back to amorphous carbon, thus verifying the existing of amorphous carbon in the pre-deposited buffer layer [25,26]. Furthermore, the degree of diamond crystallization is different for the different diamond films prepared at different temperatures. This is confirmed by full width at half maximum (FWHM) of the diamond peak at 1332 cm^{-1} as presented in a magnified view in Fig. 2b. The values of the FWHM at deposition temperatures of 900, 920, 940 and 960 °C were 14.98, 6.20, 4.95 and 6.62 cm^{-1}, respectively, showing a high degree of crystallization at high temperature. The reason why the values of FWHM at 960 °C is bigger than the value at 940 °C, may be attributed to stress induced by overlapping diamond plates in the diamond film.

Fig. 3 displays the XRD spectra of diamond films deposition at 900, 920, 940 and 960 °C. For 900 °C, diamond peaks of D-111, D-220, D-311 can be observed in the XRD spectrum, which are induced by the nano-crystalline diamond grains in the amorphous carbon buffer layer. D-400 peak is very weak and hardly found in the spectrum. However, the peaks of D-400 are obvious in the XRD spectra of diamond films prepared at 920, 940 and 960 °C, verifying the deposition of 100-oriented diamond on the amorphous buffer layer.

It is intriguing that single crystal diamond plates appeared at the top of the octahedrons-shaped clusters after increasing the deposition temperature. In order to reveal the formation mechanism of the plates, cross-sectional SEM and TEM characterization were conducted for a single diamond plate on the diamond film deposited at 960 °C, since the plates formed at 960 °C have the largest average size. The cross-sectional TEM sample was in-situ prepared on the diamond film deposited using FIB. Fig. 4a shows the cross-sectional SEM image of the single diamond plate. It can be observed that single crystal diamond has been deposited on the buffer layer. Fig. 4b reveals the cross-sectional TEM image at low magnification. There are two different diffraction contrasts in the sample. Selected area electron diffraction (SAED) of the upper region displays a typical single crystal diffraction pattern of diamond cubic structure along [011] direction. In contrast, the counterpart of the lower region shows a diffraction circle of diamond {111} planes, verifying the existing of nano-crystalline diamond in the buffer layer. To observe these regions clearly, a magnified TEM micrograph of the violet square (Fig. 4b) is given in Fig. 4c. At the top of sample, a contrast typical for a single crystal can be seen. However, there is a typical nano-crystal contrast at the bottom and many nano-crystalline grains can be identified in this region. In order to further confirm the respective microstructures, HR-TEM characterization was utilized. Fig. 4 d-f present the corresponding HR-TEM micrographs of the areas highlighted in Fig. 4c. Fig. 4d clearly shows that two nano-crystalline diamond grains were embraced by amorphous carbon in the region marked by an orange circle in Fig. 4c. Their grain sizes are about 8.82 and 10.93 nm.

The grain size can also be calculated using the FWHM of diamond peak in the Raman spectrum. The relationship between the FWHM and the grain size can be quantitatively expressed [27],

$$L \approx \frac{70\ cm^{-1}}{w} nm$$

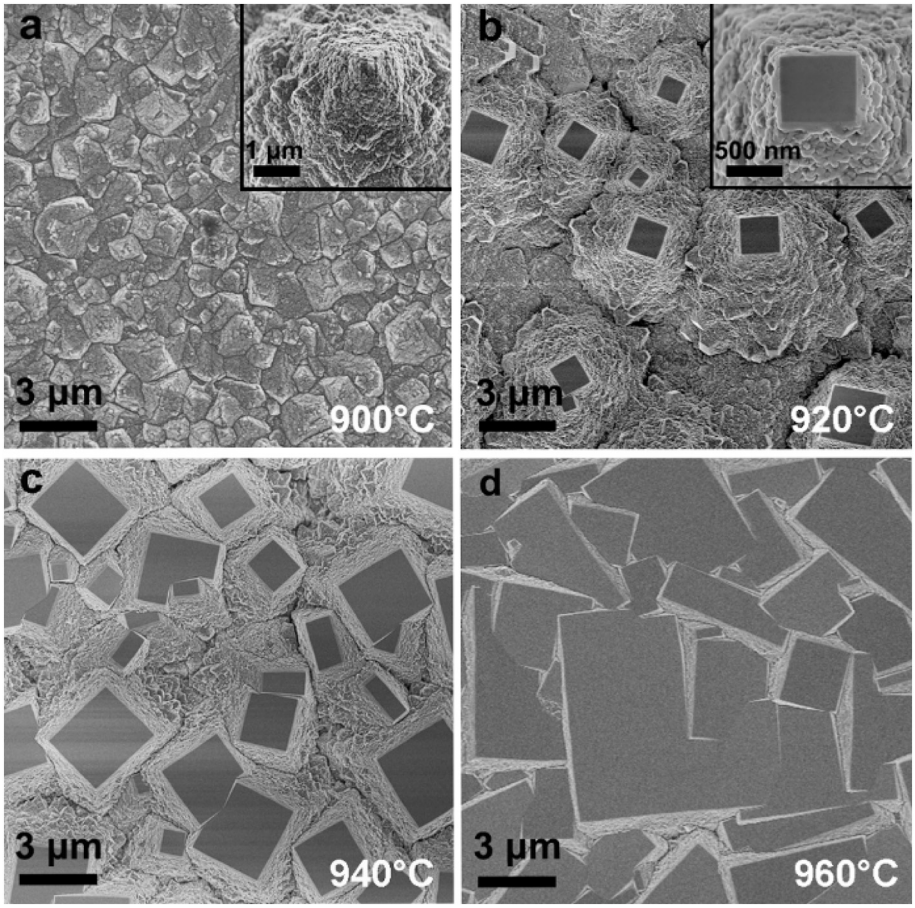

Fig. 1. SEM images of (a) pre-deposited buffer layer and diamond films prepared on the buffer layer at (b) 920 °C, (c) 940 °C and (d) 960 °C.

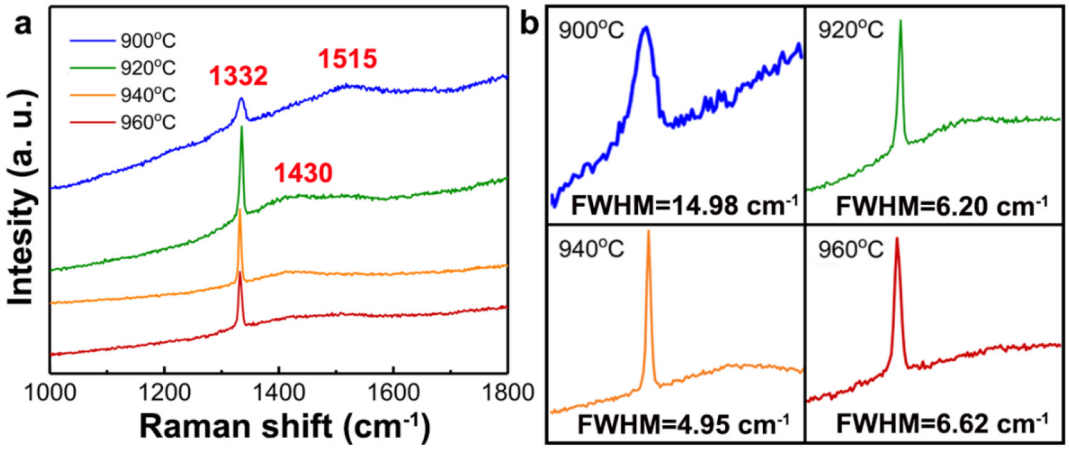

Fig. 2. Raman spectra of diamond films prepared at different temperatures.

where ω is the value of FWHM and L is the corresponding grain size. For the diamond film deposited at 960 °C, the value of the FWHM is 6.62 cm^{-1}. The calculated diamond grain size is 10.57 nm, which agrees well with TEM results. Fig. 4e displays HR-TEM micrograph of the region marked by a yellow rectangle in Fig. 4c. In this region, there is (100) oriented diamond on the amorphous carbon, confirming the direct heteroepitaxy of single crystal diamond on the amorphous carbon buffer layer. The (100)-oriented diamond film is grown from the nano-crystalline diamond grain in the amorphous carbon layer. When the deposition temperature increases, the (100) oriented diamond grain will preferentially grew up and form (100) oriented diamond film, rather than all oriented diamond grains underwent the same growth process. However, these (100) oriented nano-crystalline diamond grains have not been detected by TEM since they have the same orientation with the single crystal diamond film. Furthermore, the region marked by red ellipse in Fig. 4c shows a perfect cubic diamond structure with (100) orientation, meaning the realization of (100) oriented diamond film deposition.

Since the (100) oriented diamond film was prepared on the amorphous carbon buffer layer, it not only possesses the advantages of traditional (100) oriented diamond film, but also provides a low pore density in the diamond film. To investigate its mechanical properties, nanoindentation and scratch testing were conducted on the diamond film prepared at 960 °C. The load-displacement curve is shown in

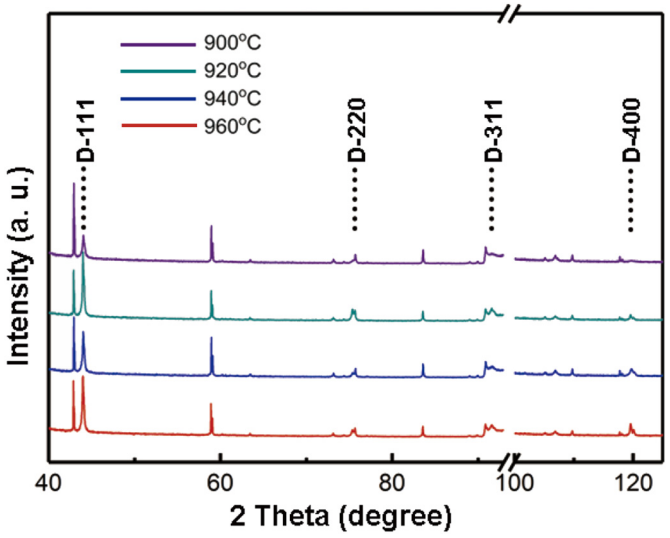

Fig. 3. XRD spectra of diamond films deposited at different temperatures.

Fig. 5a. The calculated hardness and Young's modulus were only 13.8 and 328 GPa, respectively, which are much lower than the counterparts of traditional diamond film [28]. From Fig. 5b, it can been seen that the diamond film has a friction coefficient of 0.19, which is consistent with the result in previous research [29]. In virtue of the low pore density and the existing of amorphous carbon in the prepared (100) oriented diamond film, it would possess a high toughness. Combining the high strength of single crystal diamond, the (100) oriented diamond film with a unique structure comprising amorphous carbon buffer layer and single crystal diamond, will be a promising material overcoming the brittleness of traditional (100) oriented diamond film.

4. Conclusions

In summary, diamond films were prepared on pre-deposited amorphous carbon buffer layers. SEM and Raman shift were employed to characterize the surface morphology as well as the quality of buffer layer and diamond film. Cross-sectional SEM and TEM results demonstrated that (100) oriented diamond film directly grows on the amorphous carbon buffer layer, thus leading to the formation of single crystal diamond plate. HR-TEM observation of the interface between buffer layer and single crystal diamond indicates that the formation of (100) oriented diamond film is attributed to the fast lateral growth of nano-crystalline diamond grains with (100) orientation in the amorphous carbon buffer layer.

Author contributions section

B. Wang and N. Jiang conceived the projects. B. Wang and Y. X. Lu wrote the paper. B. Wang, W. D. Man and Y. X. Lu performed the deposition and characterization of the diamond films. B. Wang, Y. X. Lu and N. Jiang carried out the FIB and TEM experiments. All authors discussed the results and commented on the manuscript.

Declaration of competing interest

The authors declare that they have no known competing financial interests or personal relationships that could have appeared to influence the work reported in this paper.

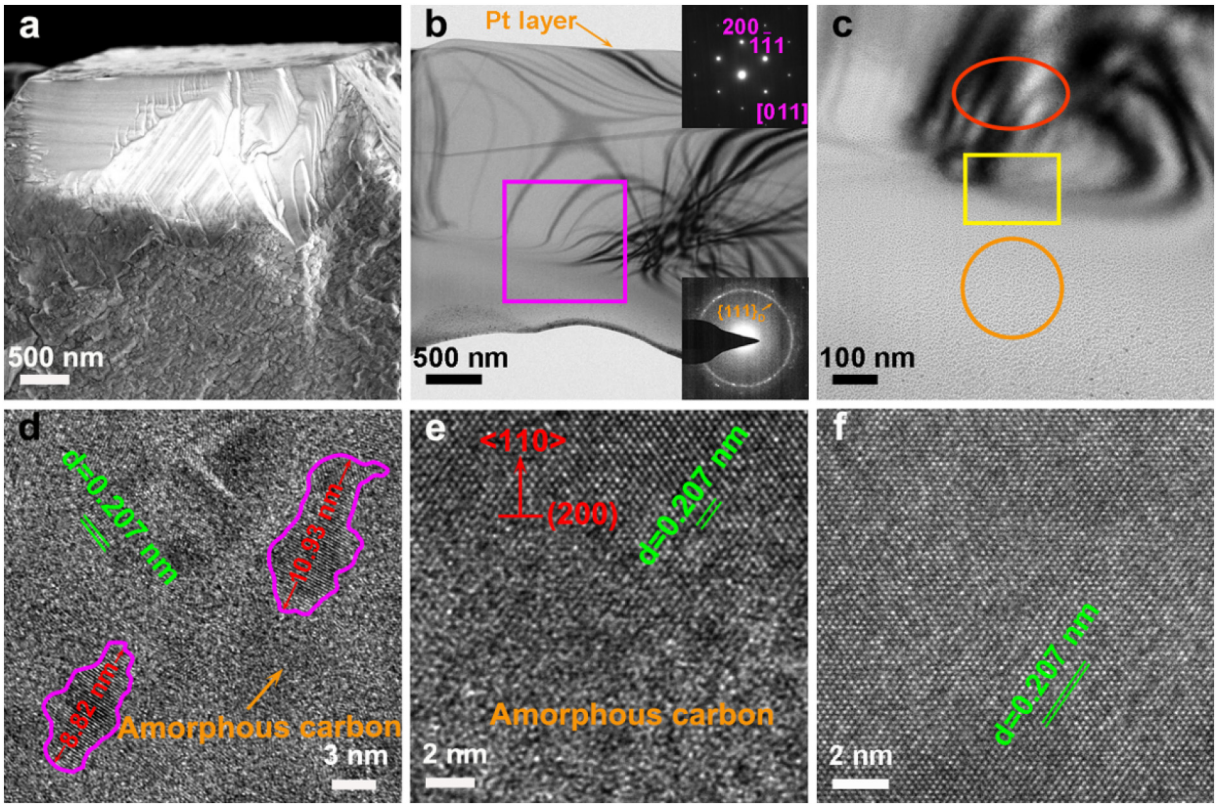

Fig. 4. Cross-sectional (a) SEM image and TEM micrographs at (b) low magnitude, (c) enlarged image marked by a violet square in Fig. 4b, and high resolution TEM micrographs of the areas marked by (d) orange circle, (e) yellow rectangle and (f) red ellipse in Fig. 4c. (For interpretation of the references to color in this figure legend, the reader is referred to the web version of this article.)

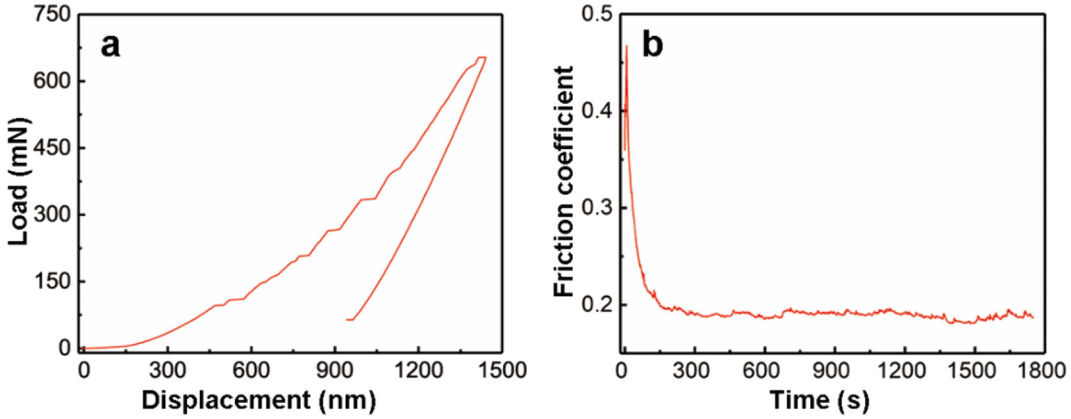

Fig. 5. Nanoindentation and friction testing of the diamond film deposited at 960 °C under the load of 2 N.

Acknowledgement

The authors are grateful for the financial support by the National Key Research and Development Project (2017YFE0128600), Ningbo 3315 Innovation Team (Y90331DL02), Science and Technology Innovation 2025 Major Project of Ningbo (2018023), National Defense Key Laboratory Fund (6142807180511), '13th Five-Year' Equipment Pre-research Sharing Project (E1710161) and 'Key Talents' Senior Engineer Project of Ningbo Institute of Materials Technology and Engineering. A. R. greatly acknowledges the financial support of CONICYT (FONDECYT 11180121).

References

[1] Q. Wang, J. Bai, B. Dai, L. Yang, P. Wang, Z.H. Yan, S. Guo, Y.M. Zhang, J.C. Han, J.Q. Zhu, Morphology-controllable synthesis of highly ordered nanoporous diamond films, Carbon 129 (2018) 367–373.
[2] X.J. Liu, P.F. Lu, H.C. Wang, Y. Ren, X. Tan, S.Y. Sun, H.L. Jia, Morphology and structure of Ti-doped diamond films prepared by microwave plasma chemical vapor deposition, Appl. Surf. Sci. 442 (2018) 529–536.
[3] R. Tu, T.T. Xu, D.F. Li, S. Zhang, M.J. Yang, Q.Z. Li, L.M. Zhang, T. Shimada, T. Goto, J. Shi, Morphology and mechanical behavior of diamond films fabricated by IH-MPCVD, RSC Adv. 8 (2018) 16061.
[4] D.H. Xiang, Y.B. Chen, Z.H. Guo, H.R. Feng, B.F. Wu, X.X. Niu, Influence of textured diamond film on tribological properties of cemented carbide substrate, Int. J. Refract. Met. H. 78 (2019) 303–309.
[5] V.V. Mitic, H.J. Fecht, M. Mohr, G. Lazovic, L. Kocic, Exploring fractality of microcrystalline diamond films, AIP Adv. 8 (2018) 075024.
[6] T. Izak, T. Sakata, Y. Miyazaw, T. Kajisa, A. Kromka, B. Rezek, Diamond-coated field-effect sensor for DNA recognition—influence of material and morphology, Diam. Relat. Mater. 60 (2015) 87–93.
[7] S. Talu, M. Bramowicz, S. Kulesza, A. Ghaderi, V. Dalouji, S. Solaymani, M.F. Kenari, M. Ghoranneviss, Fractal features and surface micromorphology of diamond nanocrystals, J. Microsc. 264 (2016) 143–152.
[8] Y.J. Wang, J.X. Li, H.Y. Long, H. Luo, B. Zhou, Y.N. Xie, S.S. Li, Q.P. Wei, Z.M. Yu, A periodic magnetic field assisted chemical vapor deposition technique to fabricate diamond film with preferred orientation, Surf. Coat. Tech. 292 (2016) 49–53.
[9] Q.F. Su, Y.B. Xia, L.J. Wang, J.M. Liu, W.M. Shi, Optical and electrical properties of different oriented CVD diamond films, Appl. Surf. Sci. 252 (2006) 8239–8242.
[10] C.C. Wang, X.C. Wang, F.H. Sun, Tribological behavior and cutting performance of monolayer, bilayer and multilayer diamond coated milling tools in machining of zirconia ceramics, Surf. Coat. Tech. 353 (2018) 49–57.
[11] W.C. Lai, Y.S. Wu, H.C. Chang, Y.H. Lee, Differing morphologies of textured diamond films with electrical properties made with microwave plasma chemical vapor deposition, Appl. Surf. Sci. 257 (2010) 1729–1735.
[12] A. Bogatskiy, J.E. Butler, A geometric model of growth for cubic crystals: diamond, Diam. Relat. Mater. 53 (2015) 58–65.
[13] J. Weng, J.H. Wang, S.Y. Dai, L.W. Xiong, W.D. Man, F. Liu, Preparation of diamond films with controllable surface morphology, orientation and quality in an over-moded microwave plasma CVD chamber, Appl. Surf. Sci. 276 (2013) 529–534.
[14] I.H. Choi, P. Weisbecker, S. Barrat, E. Bauer-Grosse, Growth of highly oriented diamond films by the MPCVD technique using CO-H_2, CH_4-H_2 and CH_4-N_2-H_2 gas mixtures, Diam. Relat. Mater. 13 (2004) 574–580.
[15] Y.K. Kim, J.Y. Lee, Formation of highly oriented diamond film on (100) silicon, J. Appl. Phys. 81 (1997) 3660–3666.
[16] S.D. Wolter, T.H. Borst, A. Vescan, E. Kohn, The nucleation of highly oriented diamond on silicon via an alternating current substrate bias, Appl. Phys. Lett. 68 (1996) 3558–3560.
[17] S.M. Yang, Z.T. He, Q.T. Li, D.Z. Zhu, J.L. Gong, Diamond films with preferred ⟨110⟩ texture by hot filament CVD at low pressure, Diam. Relat. Mater. 17 (2008) 2075–2079.
[18] T. Suto, J. Yaita, T. Iwasaki, M. Hatano, Highly oriented diamond (111) films synthesized by pulse bias-enhanced nucleation and epitaxial grain selection on a 3C-SiC/Si (111) substrate, Appl. Phys. Lett. 110 (2017) 062102.
[19] N. Yokonaga, Y. Katsu, T. Machida, T. Inuzuka, S. Koizumi, K. Suzuki, Oriented growth of diamond on thermally carburized silicon substrates, Diam. Relat. Mater. 5 (1996) 43–47.
[20] A. Flöter, H. Güttler, G. Schulz, D. Steinbach, C. Lutz-Elsner, R. Zachai, A. Bergmaier, G. Dollinger, The nucleation and growth of large area, highly oriented diamond films on silicon substrates, Diam. Relat. Mater. 7 (1998) 283–288.
[21] C. Delfaure, N. Tranchant, J.P. Mazellier, P. Ponard, S. Saada, Monitoring texture formation during diamond growth by specular and diffuse reflectance interferometry, Diam. Relat. Mater. 69 (2016) 214–220.
[22] G.F. Zhang, V. Buck, A simple method to grow textured (111) diamond thin films in a hot-filament CVD system, Appl. Surf. Sci. 207 (2003) 121–127.
[23] N. Bozzolo, S. Barrat, I. Dieguez, E. Bauer-Grosse, Crystalline quality of highly oriented diamond films grown on (100) silicon studied by conventional TEM, Diam. Relat. Mater. 6 (1997) 41–47.
[24] A.J.S. Fernandes, M.A. Neto, F.A. Almeida, R.F. Silva, F.M. Costa, Nano- and microcrystalline diamond growth by MPCVD in extremely poor hydrogen uniform plasmas, Diam. Relat. Mater. 16 (2007) 757–761.
[25] P.V. Huong, Structural studies of diamond films and ultrahard materials by Raman and micro-Raman spectroscopies, Diam. Relat. Mater. 1 (1991) 33–41.
[26] J. Stiegler, T. Lang, M. Nyggtrd-Ferguson, Y. Kaenel, E. Blank, Low temperature limits of diamond film growth by microwave plasma assisted CVD, Diam. Relat. Mater. 5 (1996) 226–230.
[27] P.K. Bachmann, D.U. Wiechert, Optical characterization of diamond, Diam. Relat. Mater. 1 (1992) 422–433.
[28] S. Chowdhury, E. de Barra, M.T. Laugier, Hardness measurement of CVD diamond coatings on SiC substrates, Surf. Coat. Tech. 193 (2005) 200–205.
[29] Q.H. Fan, E. Pereira, P. Davim, J. Gracio, C.J. Tavares, Friction and adhesion behavior of polycrystalline diamond films deposited on metals, Surf. Coat. Tech. 126 (2000) 110–115.